Material characterization and failure envelope evaluation of filament wound GFRP and CFRP composite tubes

Giovanni Perillo[1*], Robin Vacher[1], Frode Grytten[2], Steinar Sørbø[3], Virgile Delhaye[1]

[1] *SINTEF Material and Chemistry Department of Material and Structural Mechanics – N-7491 Trondheim – Norway*
[2] *SINTEF Material and Chemistry Department of Polymer and composite materials– Oslo – Norway*
SINTEF Raufoss Manufacturing – Raufoss – Norway

Abstract

The full procedure for material characterization of filament wound composite pipe is here reported and investigated. Two different typologies of composite were used in order to evaluate the goodness of the developed test methodology. Testing samples were produced with glass/vinylester and carbon/epoxy in tubular section by filament winding process.
Split disk and biaxial tests were used to evaluate the basic in plane material properties. A new design for the biaxial test was developed. The end tabs and fixture were made in order to reduce the stress concentration at the edges of the samples and to remove any possibility of sample misalignments. The influence of the sample length as well as the sample preparation was investigated and the best solution reported. Moreover an innovative optical method was developed for the evaluation of the void content of the produced material.
In addition to the basic strength data, the complete failure envelopes in the plane $\sigma_2 - \tau_{12}$ were also evaluated for both materials by the use of the biaxial test procedure here developed. The experimental failure envelopes were also compared with the prediction made with some of the most common failure theories currently available. The results clearly showed the goodness of Puck criterion to accurately predict the failure envelope (especially when torsion plus axial compressive loads were applied to the samples).

Keywords: *Filament Winding Pipe, Material Properties, Biaxial Test, Split Disk Test*

1. Introduction

In the last decade, the use of filament wound composite materials has drastically increased especially when high strengths and good corrosion properties are required. Filament wound composites have been replacing metal alloys in several applications, for example high-pressure vessel in chemical plant or aeronautical/space vehicles, or transportation tubes in oil, gas and nuclear industry, or trusses for tubular structures [1].
The massive use of composites produced by filament winding is increasing the demand for advanced and specialized testing techniques in order to properly characterize the material behaviour/properties. Over the years several methods have been developed to test filament wound component. The ISO 1268-5 standard [2] describe the procedure to produce flat panel by filament winding allowing the use of the classical testing technique developed for flat composites samples. This approach, even if widely used for industrial applications, presents several drawbacks [1]. Interlaminar stresses occur at the free edge of a sample and can lead to the premature failure of the sample inducing the so call 'edge effect' [1]. Moreover the absence of the optimal compaction (due to the winding on flat surface instead of curved one) can produce higher void content and lower fiber fraction compared to those of actual components in filament wound material [3]. For these reasons specialized test methods for tubular/ring samples, have been developed and standardized by ASTM organization [4-7].

*Correspindign author - Email: giovanni.perillo@sintef.no Telephone number: (+47) 47160974

In the current work, the complete testing procedure for the material characterization of filament wound composite material is reported and analysed in details. Both E-Glass/Vinylester and Carbon/Epoxy composites were tested in order to evaluate the applicability of the test method to both material systems/fibre types. Two different test methods were used. Ring samples were tested according to the split disk test procedure [4] to evaluate the properties in the fibre direction (both modulus and strength). Biaxial tests [5-7], with the combined axial plus/torsional load, were carried out on tubular samples. The material moduli and strengths were evaluated in the direction transverse to the fibre in addition to the shear data. A new design for the fixture and end tabs was developed in order to minimize the stress concentration effect at the side (end) of the tubular sample.
The biaxial test techniques reported in the ASTM standards [5-7] give the possibility to evaluate the material data when uniaxial axial load conditions are applied to the sample. But all the real structures are subject to complex load conditions resulting in biaxial or tri axial states of stress [8]. For this reason the main challenge for the designer is to predict the material failure (from the uniaxial strength data) when multi axial stress conditions are applied to the structure. In these conditions failure theories are generally used to predict the damage. These are mathematical functions, based on experimental or theoretical basis, which predicts the material failures under complex stress condition using the experimental strength data. In the last thirty years, several failure theories have been published. Among them Hashin [9, 10], Tsai-Wu [11], Tsai-Hill [12] and the most recent Puck [13, 14] have been widely used.
The developed biaxial test configuration was here used to experimentally evaluate the complete failure envelope in the plane $\sigma_2 - \tau_{12}$. This was then compared with the theoretical envelope predicted using the failure theories in order to evaluate their accuracy.

2. Methodology

2.1. Used material

In order to evaluate the goodness of the developed test procedure, two different types of filament wound composites were characterized. The used materials presented differences in both the main constituents and production parameters (more details in the following sections).

Glass Fibre Reinforced Polymer

Glass Fibre Reinforced Polymer (GFRP) pipes were manufactured using Advantex™ E-Glass fibres supplied by 3B (bobbins for direct roving) and Dion 9100-61 + Norpol Nr 24 vinylester system (mix ratio of 100:2 by weight). All pipes were manufactured using a computer-controlled 4 axes filament winding machine (MAW 20 LS 4/1 by Mikrosam). During the production, the tension of the fibre tows was monitored and kept constant (20N) using a computer based tensioning system. The pipes were produced on a steel mandrel covered by a PVC pipe (to prevent any damage on the mandrel during the extraction). Before starting the production, the PVC pipe was covered by a thick layer of mold release agent (Chemlease 2185 + Renlease QV5110) to facilitate the mandrel extraction. After the winding, the pipes were cured at room temperature for 24h, and then post cured at 100° for 1.5h. The samples were produced in long pipe of approximately 1500 mm and then cut according to the final samples length. All the samples were accurately examined to verify the absenceof delamination close to the cut edges.

Carbon Fibre Reinforced Polymer

Carbon fibre reinforced polymer (CFRP) pipes were manufactured using TCR™ high performance towpreg. Toray M30SC Carbon Fibre 18k and TCR UF3325 epoxy resin were the main constituents of the used prepreg. A fully automated 4 axes filament winding machine, produced by Bolenz & Schäfer GmbH, was used for the material production. The fibre tension was monitored and kept constant at 20N during the production by the use of computer controlled tensioning system. The prepreg band of 3mm width, were winded over a steel mandrel covered with mold release agent. Several pipes were produced with an approximately length of 800mm. After winding, the pipes were cured in two different steps: before 2h at 100 °C

and then 4h at 140 °C. The samples were then cut according to the final sample length using a diamond pipe sow. All the samples were accurately checked to verify the absence of delamination or any other type of damage near the cut edges.

All the pipes (for both materials) were produced with a pure hoop layup (approximately 89°, function of the used band width). The winding quality was verified for each produced pipe by comparing the fibre and void contents (more details in the following sections).

2.2. Split disk test

The longitudinal properties in the fibre direction (E_1 Young's modulus and X_t tensile strength), were evaluated by the split disk test following the general suggestions of the ASTM D2290 standard [4]. All the tests (for both materials) were carried out in a hydraulic INSTRON 10 Ton machine and recorded by a digital acquisition system at a sampling rate of 4Hz. All the tests were done in displacement control at a constant displacement of 0.5mm/min. A customized design for the fixture was developed (more details in Figure 1).
The samples presented a pure hoop layup with an internal diameter of 50.0±0.5mm, width of 10.0±0.5mm and thicknesses of 1.2±0.1mm for GFRP 1.7±0.1mm for the CFRP. The sample width was defined in order to have at least two bands of fibre in the width of the sample (band width of approximately 4mm for the GFRP and 3mm for CFRP). This reduced the possible influence of local material imperfection on the obtained results. The thickness instead was chosen in order to obtain the best compromise between: the number of overlapped layers and the final sample thickness. The increase of the overlapped layers of fibre was necessary in order to guarantee a homogeneous coverage of the mandrel (affected by the possible variation of the fibre band width during the production). On the other hand, there was the necessity to keep a lower material thickness in order to not overcome the design load of the fixtures.
A total of 20 samples for GFRP and 15 for CFRP were tested (less samples for CFRP due to the material limitation). Ten samples for each material were also equipped, according to Yoon [15], with one unidirectional strain gauge to evaluate the elastic modulus (E_1). As suggested in [15], the strain gauges were placed in the part of the sample directly in contact with the fixture (see Figure 1) in order to avoid the bending effect of the middle part of the sample. In order to reduce the effect of the friction, liquid lubricant was applied on the fixture surface (contact part with the sample).
The elastic modulus E_1 was calculated by the evaluation of the slope in the linear part of the stress-strain curves (from strain gauge). The strength instead was calculated according to the ASTM D2290 [4] by the Eq. 1.

$$X_t = \frac{P}{2A_{max}} \qquad \textbf{Eq. 1}$$

Where

X_t=Ultimate tensile strength [MPa]
P= maximum load [N] evaluated by the machine (load cell) data
A_{max}= minimum cross sectional area of the sample [mm^2]

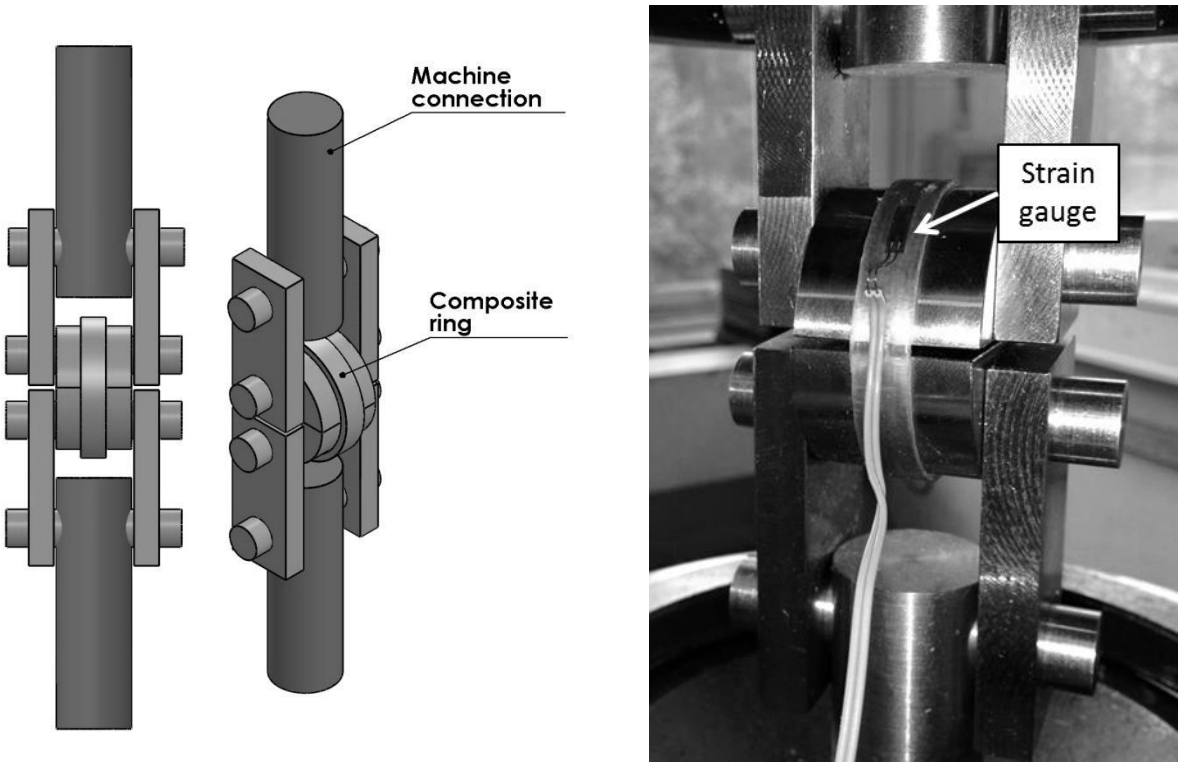

Figure 1: Split disk test fixture with the strain gauge positioning

2.3. Biaxial tests

The material properties in the direction transverse to the fibre (E_2 modulus, Y_t tensile strength, Y_c compressive strength) in addition to the shear modulus (G_{12}) and strength (S_{12}) were tested using filament wound tubular samples by an hydraulic multi axes (axial or/plus torsional loads) test machine INSTRON 8550. In addition to the basic material properties, the complete failure envelopes in the plane $\sigma_2 - \tau_{12}$ were also evaluated for both materials. The experimental failure envelopes were then compared with some of the most popular failure theories in order to evaluate their capabilities to predict the damage under complex multi-axial loading conditions.

Sample dimension and preparation

During the preliminary test phase, it was observed that several parameters (as sample's geometry, end tabs, fixture and sample preparation) played a critical role in order to obtain the correct damage.

The sample dimensions were initially defined according to the suggestions provided by Whitney et al. [16] and Vicario et al. [17] to design thin walled filament wound tubular specimens. According to their suggestions, the sample radius divided by the length (R/L) should be less than 0.1, while the radius divided by the thickness (R/t) should be higher than 10. The samples used in this work, presented an internal diameter of 50mm and length of 120mm with a thickness 2.4±0.2mm for GFRP and 1.7±0.1mm for CFRP. These dimensions only partially fulfilled the suggestions reported before, resulting in $R/L = 0.2$ (suggested <0.1) with $R/t = 10.4$ for GFRP and $R/t = 14.7$ for CFRP (suggested >10). As reported by Mistry et al. [18], the increase of the R/L ratio can result in a higher influence of the end fitting with more sensitivity to the axial load. For this reason several preliminary tests were done in order to evaluate the influence of the sample length (with the designed end tabs – more detail after) to the axial load. The results showed that a decrease of the samples length (with the consequent increase of the R/L ratio) did not affect significantly the results. Due to the limited amount of available material, the reduction of the sample length resulted in the possibility to perform more tests.

An customized design was developed for the machine fixtures in order to prevent any sample misalignment and any source of stress concentration. Schematic drawings of the sample and fixture geometries are shown in Figure 3. The end tabs were designed to reduce the production cost (important due to the impossibility to re-use the tab after the test) and provide a fast sample alignment with the possibility of using different samples thickness. The tabs were designed with a trapezoidal section providing a precise and fast sample alignment and leaving the required space for the glue (the details drawings are reported in Figure 3.c). The tabs were optimized to be produced in aluminium by lathe (speeding up the production).
The preliminary test phase clearly highlighted the crucial importance of the glue (between the tabs and sample) in order to obtain the correct results/failure mode. Several different types of epoxy based glues were tested. The best results were obtained using structural bi-components epoxy based glue Araldite 2015 cured for 15h at 40°C. The selected glue, specific for metal composite bonding, provided the required strengths coupled with the ability to fill the small gap between the sample and the tab. After the application of the glue, the tabs and the sample were aligned using an internal tube (covered with a non-stick Teflon layer).
Even with all the expedients previously reported, the samples preparation was time consuming and needed a lot of experience in order to obtain good results. A total of 22 samples of GFRP and 33 of CFRP were prepared and tested.
All the samples were equipped with unidirectional or three axial strain gauges according to the specific tests type:

- Pure axial load (tension or compression): 2/3 UD strain gauges around the sample midsection (according to the ASTM D5450 [5]/ASTM D5449 [6])
- Pure torsional load: 2 three-axial (rosette) strain gauges placed at 180° around the sample midsection (according to ASTM D5448 [7])
- Multi-axes loads: 2/3 UD strain gauges around the sample midsection

Load configurations
In order to evaluate the complete failure envelope (in the plane $\sigma_2 - \tau_{12}$) in addition of the basic material properties, four combinations of axial and/or torsional loads were tested:

- ***Pure axial load****:* pure axial load (tension or compression) was applied until the final failure. The torsion was monitored and kept at zero.
- ***Pure shear****:* pure torsion was applied to the samples until the final failure. The axial load was monitored and kept at zero.
- ***Shear + axial load****:* pure torsion was applied to the sample up a to a fixed value. Subsequently, the axial load (tension or compression) was applied until the final failure (keeping the torsion load constant).
- ***Axial load + shear****:* pure axial compression or tension load was applied to the sample up a to a fixed value. Subsequently, torsion was applied until the final failure (keeping the axial load constant).

Data analysis
Tension/compression modulus was evaluated using the initial linear part of the strain stress curve measured by the strain gauges. The failure strength (tension/compression) was calculated, according to the ASTM D5450 [5]/ASTM D5449 [6], by the Eq. 2:

$$Y_{t/c} = \frac{P_{max}}{A_{min}} \qquad \textbf{Eq. 2}$$

Where

$Y_{t/c}$=Ultimate tensile/compressive strength [MPa]
P_{max}= maximum load [N] (tension/compression) carried by the sample
A_{min}= minimum cross sectional area of the sample [mm^2]

The shear modulus was evaluated, according to the ASTM D5448 [7], by the Eq. 3:

$$G_{12} = \frac{\Delta_{12}}{\Delta\gamma_{12}} \quad \textbf{Eq. 3}$$

Where:

G_{12} = in plane shear modulus [GPa]

$\Delta\tau_{12}$= variation in the applied shear stress between two strain points (generally 1000με and 6000 με)

$\Delta\gamma_{12}$= difference between the two shear strain points (generally 1000με and 6000 με)

The shear strength was evaluated, according to the ASTM D5448 [7], by the Eq. 4:

$$S_{12} = \frac{T_{max}\, r_{max}}{J} \quad \textbf{Eq. 4}$$

Where:

T_{max}= the maximum torque applied to the cylinder [Nm]

J= the polar moment of inertia calculated as:

$$J = \frac{\pi}{32}(OD^4 - ID^4) \quad \textbf{Eq. 5}$$

OD= Outer diameter ID=Inner diamiter

r_{max}= the maximum radial distance ($r_{max} = OD/2$)

2.4. Failure Envelope ($\sigma_2 - \tau_{12}$)

The experimental failure envelopes in the plane $\sigma_2 - \tau_{12}$ were compared with some of the classical failure theories used for composite materials. A short summary of the used theories is reported here. All the equations are reported assuming the stresses in the fibre direction $\sigma_1 = 0$, with σ_2 the stress in the transverse direction and τ_{12} the shear stress.

Max Stress criterion [19]

This criterion assumes no interaction between the different failure modes. The damage is predicted when one of the follow criteria is verified:

$$\begin{cases} \sigma_2 \geq Y_t \quad for \;\; \sigma_2 < 0 \\ \sigma_2 \geq Y_c \quad for \;\; \sigma_2 > 0 \\ \tau_{12} \geq S_{12} \end{cases} \quad \textbf{Eq. 6}$$

Tsai – Wu [11]

This is a quadratic interaction failure criterion in which all the strength data are used to create the failure surface. The failure is predicted when the following equation is verified.

$$\left(\frac{1}{Y_t} - \frac{1}{Y_c}\right)\sigma_2 + \frac{\sigma_2^2}{Y_t Y_c} + \left(\frac{\tau_{12}}{S_{12}}\right)^2 \geq 1 \quad \textbf{Eq. 7}$$

Tsai – Hill [12]

This criterion distinguishes between the different failure modes and it is based on a modified version of the yield criterion for metals.

$$\left(\frac{\sigma_2}{Y^2}\right) + \frac{\tau_{12}}{S_{12}^2} \geq 1 \qquad \begin{matrix} Y = Y_t \;\; for \;\; \sigma_1 > 0 \\ Y = Y_c \;\; for \;\; \sigma_1 < 0 \end{matrix} \quad \textbf{Eq. 8}$$

Hashin 1973 [10]

This is a stress based failure criterion developed for unidirectional composite.

$$\begin{cases} \left(\frac{\sigma_2}{Y_t}\right)^2 + \left(\frac{\tau_{12}}{S_{12}}\right)^2 \geq 1 \quad for \quad \sigma_2 > 0 \\ \left(\frac{\sigma_2}{Y_c}\right)^2 + \left(\frac{\tau_{12}}{S_{12}}\right)^2 \geq 1 \quad for \quad \sigma_2 < 0 \end{cases} \qquad \textbf{Eq. 9}$$

Puck [13, 14, 20]

Due to the complexity of the Puck [13, 14, 20] failure theory, no details are reported in the present work. More details can be found in the publications by Puck [13, 14, 20].

3. Results and discussion

3.1. Fibre volume fraction and micrograph analysis

The fibre volume fraction (V_f) was evaluated for both materials by ignition loss tests according to the ASTM D 2584 [21]. At least two samples for each of the produced pipes were tested in order to evaluate the winding quality. All the pipes showed similar V_f with a variance within ±2% (this can be considered an acceptable value for filament winding material [1]). The measured fibre volume fraction was 45.7±0.5% for the GFRP and 65.5±1% for the CFRP.
As reported by Peter [1], the void content considerably influence the transverse (to the fibre) material properties. For this reason, one sample for each of the produced pipes (GFRP and CFRP) was inspected under an optical microscope in order to have an evaluation of the void content. A representative sample for each type of composite is reported in Figure 2. Both materials showed a high quantity of voids (black spot in Figure 2). These are mainly related to the production process and are almost impossible to avoid. An automated computer based optical technique was developed in Matlab in order to get an estimation of the void content directly from the micrographic optical images of the samples. The voids were found using a Watershed transformation while fibres were found using an edge detection algorithm based on circular Hough transform. This enables one to obtain statistics about fiber radius in addition to fibre fraction. The measured void content was approximately 2% for the GFRP and 4% for CFRP.

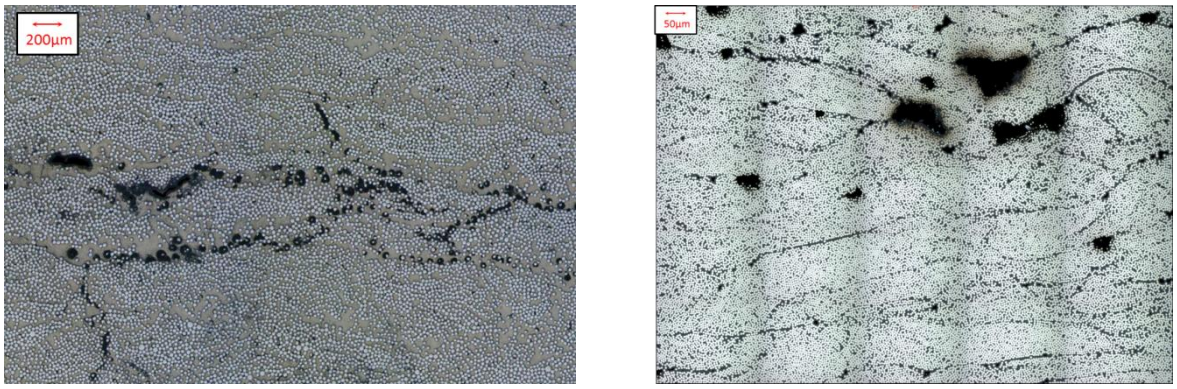

Figure 2: Optical micrograph pictures of the produced material (plane normal to the fibre direction)

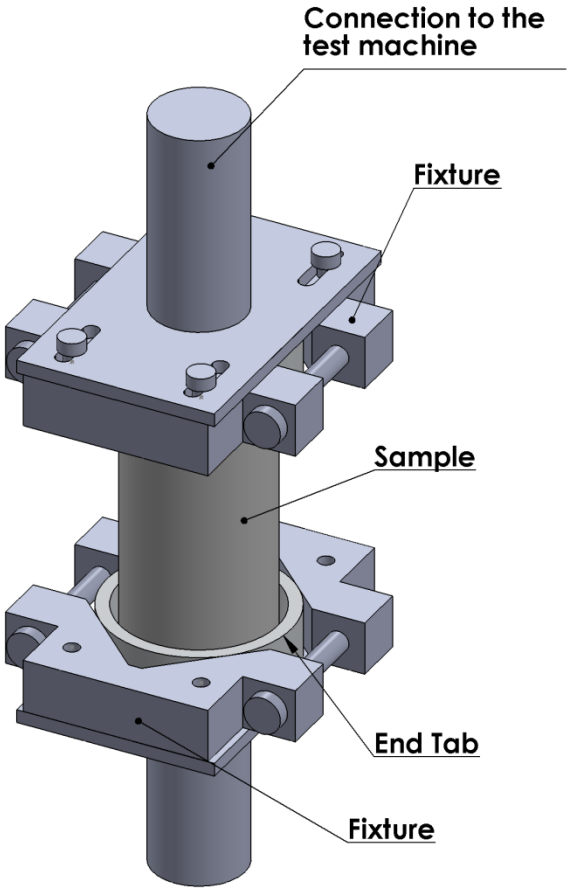

(a) Assembly

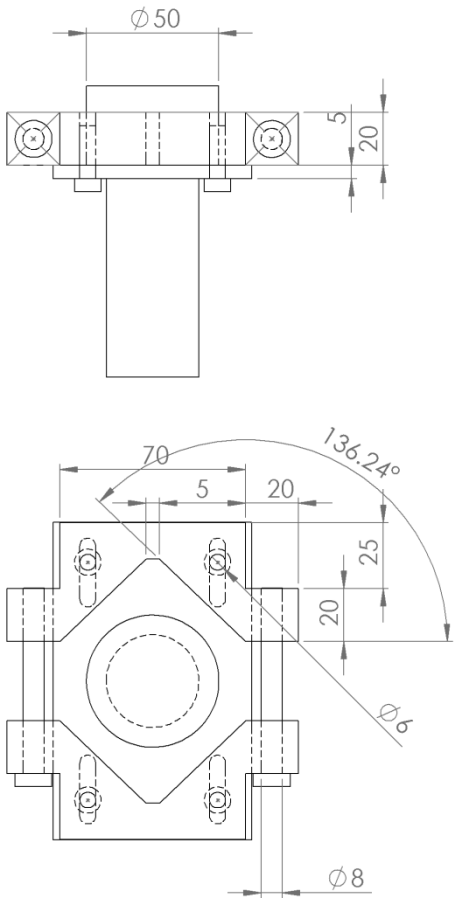

(b) Fixture

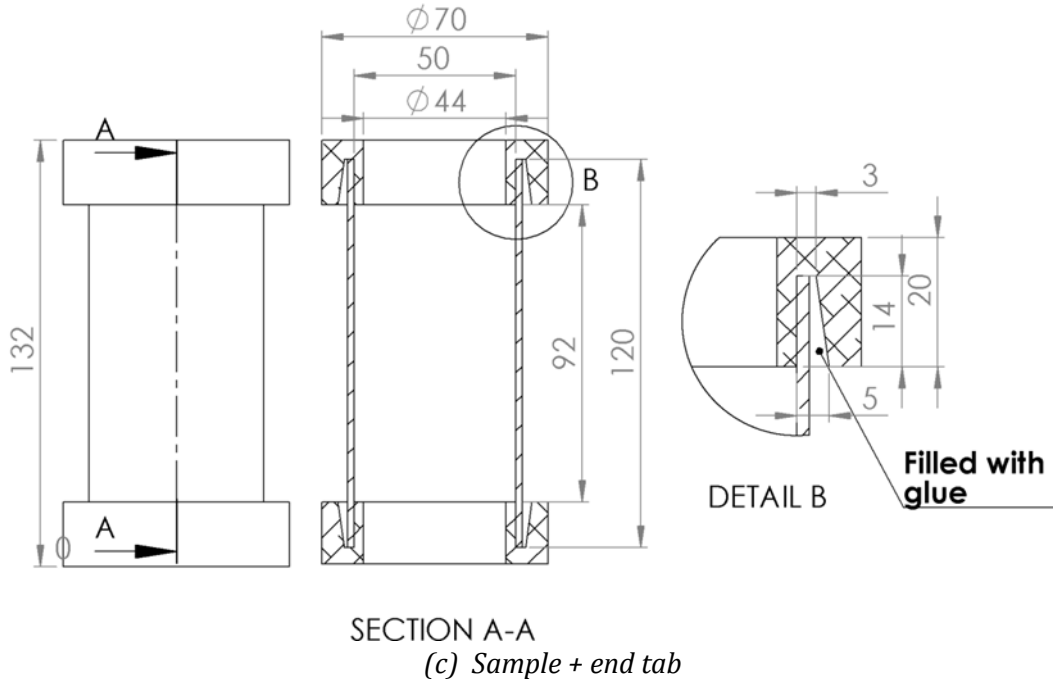

(c) Sample + end tab

Figure 3: Biaxial test geometry

3.2. Split disk tests

The results for each sample are reported in Figure 4 , Figure 5 and Table 1. The results showed a high scatter of the measured failure strength for both GFRP and CFRP composites. Both materials showed an almost linear behaviour up to the final failure. This was characterized by a loud bang with the simultaneously catastrophic damage of the samples. Furthermore in almost all the tests, even if no variations were reported in the force/displacement curves (Figure 4 and Figure 5), a noise was noticed few second before the final failure, which is a clear evidence of some damage prior to the final failure. Using a digital camera, it was possible to realize that before the final failure a long matrix crack developed along the fibre direction over the entire sample, almost dividing the sample in two different parts. A different material thickness and/or sample width could have mitigated this phenomenon. Further investigations need to be done in order to evaluate the possible influences of this problem on the results.

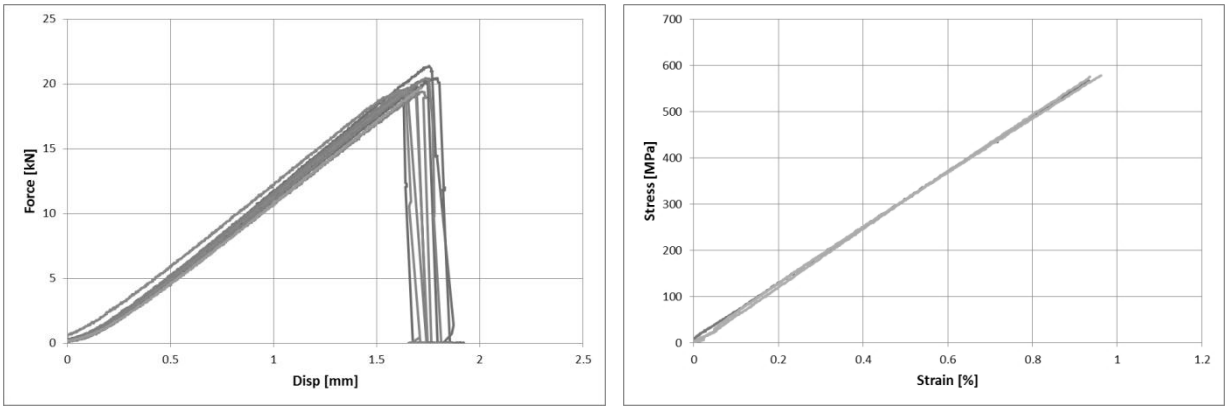

Figure 4: GFRP - Force/Disp. and Stress/Strain curve for the Split Disk Test

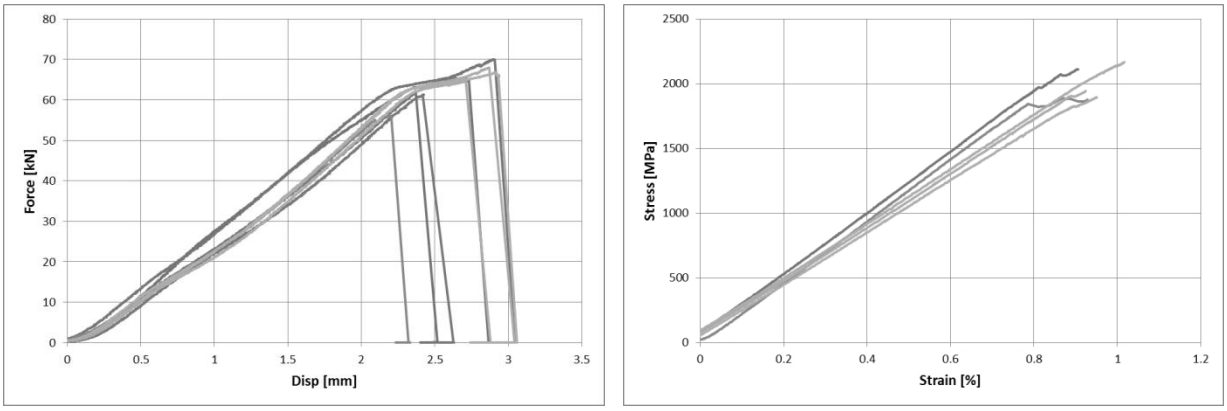

Figure 5: CFRP - Force/Disp. and Stress/Strain curve for the Split Disk Test

3.3. Biaxial tests

The results of the biaxial tests for both materials are reported in Figure 6 and Table 1. As suggested by the ASTM standards (D5450 [5], D5449 [6] and D5448 [7]), the data recorded by the different strain gauges for each sample, were compared in order to evaluate any possible misalignment. For the results reported here, this variation was within 5%. Few tests (not reported here) failed this requirement clearly showing the goodness of the designed fixtures and end tabs.

Both tested composite showed a similar behaviour. The pure tensile and compressive tests (plots not reported here) presented an almost linear behaviour up to the final failure. The damage was unexpected with no variation in the force displacement curve prior the final failure. The damage was located in the middle section (gauge section) as required by the standards. Only few samples (less than 6% of the total testes samples) showed damage in proximity of the end tab.

The test response was instead different for the pure torsional load where the samples showed a highly nonlinear behaviour up to the final failure. In this case, the failure was progressive with an accumulation of damage (mainly matrix cracks) over the whole sample. Matrix cracks where easily audible during the tests. The final failure was smooth and proceeded with a clear drop of the measured torque.
The combination of axial and torsional loads resulted instead in a mix of the two behaviours previously reported. The highly nonlinear behaviour seen for the pure torsional load, was reduced when an axial compressive load was applied to the sample. Moreover the scatter between the different tests curves was reduced when axial plus torsional loads were applied. No substantial variation were reported inverting the load application sequence (axial and then torsional load or torsional and then axial load). The curves as well as the measured material data did not show any substantial variation.
Due to the capability of the control system of the test machine, it was impossible to verify the influence of a simultaneously application of axial and torsional loads. Future investigation should be carried out to investigate the influence of the load application on the results.

Failure envelopes
In Figure 6, the experimental failure envelopes (in the plane $\sigma_2 - \tau_{12}$) were compared with the analytical predictions made with some of the most used failure theories for composite (more details in the previous section).
The failure envelope in case of tension plus torsional loads was accurately predicted by all the theories. More difficult was the evaluation of the failure envelope when compression plus torsional loads were simultaneously applied to the samples. The results showed that the Hashin/Tsai-Hill failure theories, highly underestimated the damage. More accurate results were predicted by the Tsai-Wu and Puck failure theories. Even if both theories provided quite satisfactory results, Puck's theory was able to better capture the proper drop of the shear strength increasing the axial compressive load.
The fracture surfaces of the different samples were also analysed. These results showed, according to the Puck's theory [13, 14, 20], the presence of a fracture angle (angle of the crack propagation) different than 0 (crack perpendicular to the sample surface). Due to the limited thickness of both investigated materials, it was impossible to proper evaluate the fracture angle. Further investigations, using a thicker material, are needed to evaluate the variation of the fracture angle with the σ_2/Y_c ratio according to the Puck's theory.

3.4. Discussion
The material properties measured for both two materials have been summarized in the Table 1. Almost all the measured data showed quite high scatter. This effect can mainly be related to the production process. As already reported by several authors [1, 3, 22], the filament winding process do not allow a perfect homogenous material quality, even using a computerized machine with a full control of all the production parameters. Voids, local fibre damage and local thickness variation can lead to higher scatter of the results.
Flat panel were also produced with the same constituents (for both composite) winding a unidirectional pattern over a flat mandrel according the ISO 1268-5 standard [2]. These were then tested following the classical test techniques for flat composite material [23-25].
Even if the same constituents were used, the material quality was highly affected. The fibre volume fraction was comparable but the void content was much higher for flat samples. This can be related to the lack of the optimal compaction during the production (induced by the curved surfaces of mandrel for cylindrical samples). The results showed a reduction of the measured properties (mainly for the strengths data) of around 50% compared to the tests carried out on the cylindrical samples. These results clearly showed the necessity to evaluate the material properties on the real produced material. The classical tests method for flat composite cannot be used to tests filament wound material. Cylindrical structures needs to be used instead.

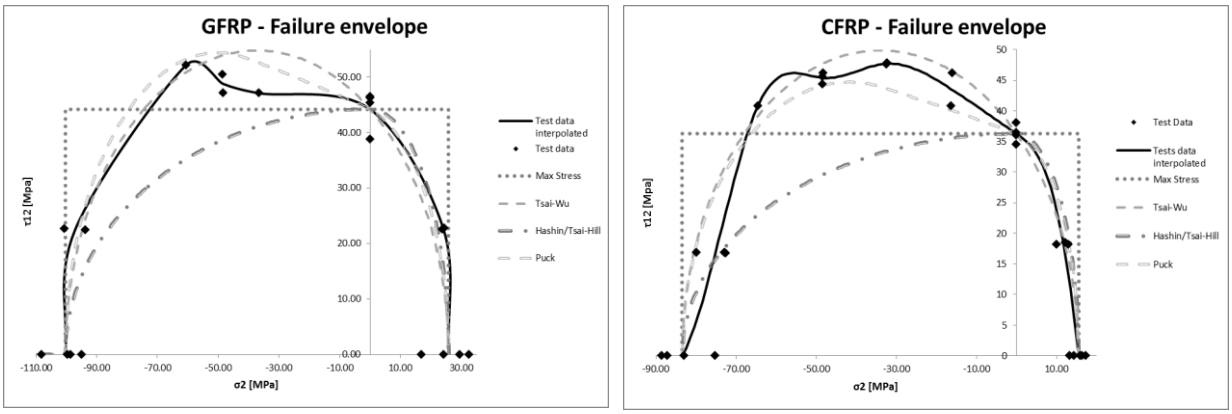

Figure 6: Failure envelopes

Table 1: Measured material properties

Properties	CFRP	CFRP
V_f	45.7 [%]	61.5 (±1) [%]
E_1	61.5 (±4.5) [GPa]	222.5 (±18.7) [GPa] Tension
X_t	837.8 (±58.0) [MPa]	1947.0 (±141.9) [MPa]
E_2	13.93 (±1.1) [Gpa] Tension 10.36 (±2.1) [GPa] Compression	7.27 (±0.5) [GPa] Tension 6.57 (±0.5) [GPa] Compression
Y_t	25.83 (±1.1) [MPa]	15.49 (±2.5) [MPa]
Y_c	100.29 (±5.0) [MPa]	83.46 (±10.3) [MPa]
G_{12}	1.43 (±0.1) [GPa]	1.7 (±0.1) [GPa]
S_{12}	44.24 (±3.1) [MPa]	36.25 (±1.3) [MPa]
ν_{12}	Assumed 0.30	

4. Conclusion

The full material characterization procedure for filament wound glass and carbon fibre composite was reported here. The different test technique were here analysed and the detailed description of the used method reported.

The capability of the split disk test to evaluate the material strength as well as the modulus in the fibre direction was demonstrated. A new design for the biaxial tests was developed. The end tabs were designed in order to facilitate the sample preparation and avoid any possibility of misalignment and stress concentration. Moreover particular attention was placed on the production cost and the versatility of the procedure (usable with different material thicknesses).

The best sample geometry was defined after a series of preliminary experimental tests varying the samples length. A higher radius/length ratio was defined for the sample compared to the suggestions provided by other authors [16, 17]. This gave the possibility to carry out more tests with the same amount of material.

The complete failure envelope, in the plane $\sigma_2 - \tau_{12}$, was also evaluated. The experimental data were compared with the prediction of some of the most common failure theories currently used. The results showed the capability of the Puck's failure theory accurately predict the complete failure envelope.

Moreover an innovative optical method for the evaluation of the void content was developed and here used with encouraging results.

Due to the increasing use of filament wound structures, further investigations should also evaluate the capability of the developed test techniques to evaluate the fatigue properties.

5. Acknowledgements

This work is part of the collaborative project "Composite structures under impact loading". The authors would like to express their thanks for the financial support by the Norwegian Research Council (grant 193238/i40) and the industrial partners. The authors would also like to thank all partners in the project for constructive discussions.

Reference

[1] Peters ST. Composite Filament Winding: Materials Park : ASM International; 2011.
[2] Standardization IOf. ISO 1268-5: Fibre-reinforced plastics -- Methods of producing test plates -- Part 5: Filament winding.
[3] Perillo G, Echtermeyer AT. Mode I Fracture Toughness Testing of Composite Pipes. Applied Composite Materials. 2013;20(6):1135-46.
[4] ASTM. D2290-12 Standard Test Method for Apparent Hoop Tensile Strength of Plastic or Reinforced Plastic Pipe.
[5] ASTM. D5450/D5450M-12 Standard Test Method for Transverse Tensile Properties of Hoop Wound Polymer Matrix Composite Cylinders.
[6] ASTM. D5449/D5449M-11 Standard Test Method for Transverse Compressive Properties of Hoop Wound Polymer Matrix Composite Cylinders.
[7] ASTM. D5448/D5448M-11 Standard Test Method for Inplane Shear Properties of Hoop Wound Polymer Matrix Composite Cylinders.
[8] Soden P, Kitching R, Tse P. Experimental failure stresses for±55 filament wound glass fibre reinforced plastic tubes under biaxial loads. Composites. 1989;20(2):125-35.
[9] Hashin. Failure criteria for unidirectional composites. J Appl Mech. 1980;47:329-34.
[10] Hashin, Rotem. A fatigue failure criterion for fiber reinforced materials. Journal of Composite Materials. 1973.
[11] Tsai. A general theory of strength for anisotropic materials. Journal of Composite Materials. 1971.
[12] Tsai. Strength characteristics of composite materials. NASA CR-224. 1965.
[13] Puck A, Schürmann H. Failure analysis of FRP laminates by means of physically based phenomenological models. Composites Science and Technology. 1998;58(7):1045-67.
[14] Puck A, Schürmann H. Failure analysis of FRP laminates by means of physically based phenomenological models. Composites Science and Technology. 2001;62(12-13):1633-62.
[15] S.-H. Yoon, W.-M. Cho, Kim C-G. Measurement of modulus in filament wound ring specimen using split disk test. Experimental Techniques. 1997.
[16] Whitney J, Pagano N, Pipes R. Design and fabrication of tubular specimens for composite characterization. Composite Materials: Testing and Design (second conference). 1971:52-67.
[17] Vicario AA, Rizzo RR. Effect of Length on Laminated Thin Tubes Under Combined Loading. Journal of Composite Materials. 1970;4:273-7.
[18] Mistry J, Gibson AG, Wu YS. Failure of composite cylinders under combined external pressure and axial loading. Composite Structures. 1992;22(4):193-200.
[19] Orifici AC, Herszberg I, Thomson RS. Review of methodologies for composite material modelling incorporating failure. Composite Structures. 2008;86(1-3):194-210.
[20] Puck A, Kopp J, Knops M. Guidelines for the determination of the parameters in Puck's action plane strength criterion. Composites Science and Technology. 2001;62(3):371-8.
[21] ASTM. D2584: Standard Test Method for Ignition Loss of Cured Reinforced Resins.
[22] Lauke B, Friedrich K. Evaluation of processing parameters of thermoplastic composites fabricated by filament winding. Composites Manufacturing. 1993;4(2):93-101.

[23] ASTM D3039 / D3039M: Standard Test Method for Tensile Properties of Polymer Matrix Composite Materials.
[24] ASTM D3410 / D3410M: Standard Test Method for Compressive Properties of Polymer Matrix Composite Materials with Unsupported Gage Section by Shear Loading.
[25] ASTM D3846: Standard Test Method for In-Plane Shear Strength of Reinforced Plastics.